AUTHOR'S QUERY SHEET

Author(s): P. Y. Lam et al. GFRR 385153
Article title:
Article no:

Dear Author

The following queries have arisen during the editing of your manuscript and are identified on the proofs. Unless advised otherwise, please submit all corrections using the CATS online correction form.

AQ1 I don't understand the 'but importantly' part of this statement – please rephrase.

AQ2 A declaration of interest statement reporting no conflict of interest has been inserted. Please confirm the statement is accurate.

Free Radical Research, Month 2009; 00(00): 1–9

informa
healthcare

Elevated neuronal nitric oxide synthase expression during ageing and mitochondrial energy production

PHILIP Y. LAM[1], FEI YIN[1], RYAN T. HAMILTON[1], ALBERTO BOVERIS[2], & ENRIQUE CADENAS[1]

[1]*Pharmacology & Pharmaceutical Sciences, School of Pharmacy, University of Southern California, Los Angeles, CA 90089, USA, and* [2]*Laboratory of Free Radical Biology, School of Pharmacy and Biochemistry, University of Buenos Aires, C1113AAD Buenos Aires, Argentina*

(Received 1 December 2008; revised 30 January 2009)

Abstract

This study evaluated the effect of ageing on brain mitochondrial function mediated through protein post-translational modifications. Neuronal nitric oxide synthase increased with age and this led to a discreet pattern of nitration of mitochondrial proteins. LC/MS/MS analyses identified the nitrated mitochondrial proteins as succinyl-CoA-transferase and F_1-ATPase; the latter was nitrated at Tyr^{269}, suggesting deficient ADP binding to the active site. Activities of succinyl-CoA-transferase, F_1-ATPase and cytochrome oxidase decreased with age. The decreased activity of the latter cannot be ascribed to protein modifications and is most likely due to a decreased expression and assembly of complex IV. Mitochondrial protein post-translational modifications were associated with a moderately impaired mitochondrial function, as indicated by the decreased respiratory control ratios as a function of age and by the release of mitochondrial cytochrome *c* to the cytosol, thus supporting the amplification of apoptotic cascades.

Keywords: *nNOS, nitration, ageing, succinyl-CoA-transferase, F_1-ATPase*

Abbreviations: *nNOS, neuronal nitric oxide synthase; SCOT, succinyl-CoA-transferase; PK, pyruvate kinase; LDH, lactic dehydrogenase*

Introduction

Nitric oxide ($^{\bullet}NO$), a free radical formed in a variety of cell types by nitric oxide synthases (NOS), is involved in a wide array of physiological and pathophysiological phenomena. The diffusibility of $^{\bullet}NO$—as an intercellular messenger—and its concentration gradients [1] in brain intra- and extracellular compartments and, hence, in pre-synaptic, synaptic and post-synaptic regions, supports its regulatory functions in brain synaptic plasticity, neurodegeneration and ageing [2–4]. The involvement of $^{\bullet}NO$ in neurodegenerative disorders, such as Alzheimer's and Parkinson's disease, is well documented: the excessive production of $^{\bullet}NO$ by the inducible form of nitric oxide synthase (iNOS) due to pro-inflammatory responses is a feature of not only neurodegenerative disorders but also brain ageing [2,4,5].

These actions of $^{\bullet}NO$ can be partly explained by the involvement of physiological concentrations of $^{\bullet}NO$ (1–100 nM) in well known cell signalling pathways: (a) its interaction with the soluble guanylate cyclase, thus yielding cGMP and resulting in signal amplification upon activation of cGMP-dependent protein kinases [6], (b) the reversible inhibition of mitochondrial cytochrome oxidase [7] and (c) protein post-translational modifications, mainly S-nitrosylation of cysteine residues [8]. When the cellular $^{\bullet}NO$ concentration exceeds the physiological levels, as in the case of induction of

Correspondence: Enrique Cadenas, Pharmacology & Pharmaceutical Sciences, School of Pharmacy, University of Southern California, Los Angeles, CA 90089, USA. Email: cadenas@usc.edu

ISSN 1071-5762 print/ISSN 1029-2470 online
DOI: 10.1080/10715760902849813

astrocyte iNOS upon pro-inflammatory responses, •NO-derived species of higher chemical reactivity (reactive nitrogen species) are generated and impair protein function [9]. Elevated •NO production and RNS formation have been implicated in the ageing process and in increased neuronal apoptosis.

The •NO-cytochrome oxidase signalling pathway referred to above is of special interest to brain ageing, because it establishes the principle of a mitochondrial redox–energy axis critical for cell function. This pathway defines a new level of regulation of mitochondrial respiration determined by the availability of ADP to F_1-ATPase and by that of O_2 and •NO to cytochrome oxidase [10]. These •NO effects on mitochondria may be accomplished by cytosol-generated •NO diffusing to mitochondria or by the activity of a mitochondrial nitric oxide synthase (mtNOS). However, the existence of a mtNOS remains controversial, despite functional evidence for a mtNOS and the report on a 144 kD nNOS variant in rat brain localized in the inner mitochondrial membrane [11,12]. Of note, the present study reports on increased cytosolic nNOS expression with age and, as mentioned above, the •NO effects on mitochondria are a function of cytosol-generated •NO diffusing to these organelles.

•NO signalling involving protein post-translational modifications becomes relevant when considering that, on the one hand, mitochondria are major sites of $O_2^{\bullet -}$ production and, on the other hand, the diffusion-controlled reaction of $O_2^{\bullet -}$ with •NO to yield peroxynitrite ($ONOO^-$) [13]. Hence, it might be surmised that mitochondrial formation of $ONOO^-$ would be favoured over the same reaction in the cytosol, considering the about one order of magnitude higher concentration of $O_2^{\bullet -}$ in mitochondria (10^{-10} M) than in cytosol (10^{-11} M) [14]. An intramitochondrial steady-state concentration of $\sim$2 nM $ONOO^-$ was calculated, taking into account the rate constants of $ONOO^-$ reactions and the concentrations of $ONOO^-$ reductants (NADH, UQH_2 and GSH) [15]. $ONOO^-$ is a strong oxidizing and nitrating species that inhibits mitochondrial NADH-ubiquinone reductase (complex I) activity [16] with implications for Parkinson's disease [17]; ATP synthase, cytochrome oxidase, aconitase and creatine kinase are inhibited by nitration or $ONOO^-$-mediated oxidation of cysteinyl residues [18–20]. $ONOO^-$ also induces mitochondrial membrane depolarization. •NO-mediated mitochondrial protein modifications (S-nitrosylation and nitration) lead to mitochondrial dysfunction, often associated with a decrease of the inner mitochondrial membrane potential and induction of mitochondrial permeability transition leading to mitochondrion-driven apoptosis triggered by cytochrome *c* release from the organelles and activation of downstream signalling apoptotic cascades [21–23].

This study was aimed at determining the effect of ageing on mitochondrial function mediated through protein post-translational modifications. It is shown that an increase in expression of cytosolic nNOS as a function of age results in a specific and discreet pattern of mitochondrial protein nitration, with implications for mitochondrial bioenergetics and mitochondrion-driven apoptosis.

Materials and methods

Animals

Fisher 344 rats of different ages (6, 14 and 26 months) were purchased from the National Institute of Ageing (NIA). Each rat was individually housed in the animal facility under standard conditions (12/12 light-dark cycle, humidity at $50 \pm 15\%$, temperature $22 \pm 2^{\circ}$C and 12 air changes/h). All procedures were approved by the local Animal Care and Use Committee.

Isolation of rat brain mitochondria

Rat brain mitochondria were isolated from adult male Fisher rats by differential centrifugation [24]. Rat brains were excised, chopped into fine pieces, washed with 0.25 M sucrose and homogenized in an isolation buffer containing 230 mM mannitol, 70 mM sucrose and 2 mM Hepes, pH 7.4, plus 0.05% (w/v) bovine serum albumin. The homogenate was centrifuged at 800 *g* for 8 min, the pellet was removed and the centrifugation process was repeated. The supernatant was centrifuged at 8000 *g* for 10 min, the pellet was washed with the isolation buffer and the centrifugation was repeated. The pellet containing a mixture of organelles was further fractionated by centrifugation at 8500 *g* for 10 min in a Percoll gradient (consisting of three layers of 18, 30 and 60% (w/v) Percoll in sucrose/Tris buffer (0.25 M sucrose, 1 mM EDTA and 50 mM Tris/HCl), pH 7.4). Mitochondria were collected from the interface of 30% and 60% Percoll and washed with the sucrose/Tris buffer. Mitochondrial protein concentration was determined using Bio-Rad protein assay dye reagent (Bio-Rad, Hercules, CA).

Detection of nNOS, cytochrome c and nitration

One hundred micrograms of mitochondrial protein were prepared in non-reducing sample buffer (Pierce, Rickford, IL), separated by 10% SDS–PAGE, electro-transferred to a polyvinylidene fluoride (PVDF) membrane and immunostained by standard methods. α-nNOS (Upstate, Lake Placid, NY), α-cytochrome *c* (Santa Cruz Biotech, Santa Cruz, CA) and α-nitrotyrosine (Upstate, Lake Placid, NY) antibodies were used to detect nNOS, cytochrome *c* and protein nitration, respectively.

Immunoprecipitation

Mitochondria isolated from 26-month old rat brains were lysed by the freeze–thaw method in RIPA buffer containing a protease inhibitor cocktail (Roche, Germany); 1 mg/ml of total mitochondrial protein was incubated with 10 μg of anti-nitrotyrosine antibody (Upstate, Lake Placid, NY) overnight at 4°C. Immune complexes were collected by incubation with protein G-agarose (Santa Cruz Biotech, Santa Cruz, CA) for 4 h at 4°C. Immunoprecipitated proteins were released from agarose by boiling in non-reducing sample buffer (Pierce, Rickford, IL), separated on 10% SDS-PAGE gel and sequenced by LC/MS/MS at the Proteomic Core Facility at the School of Pharmacy, University of Southern California.

LC/MS/MS analyses

Immunoprecipitated protein bands were excised from the gel and then subjected to in-gel tryptic digestion. Analysis of tryptic peptide sequence tags by tandem mass spectrometry was carried out as previously described [19]. Protein identification was carried out with the MS/MS search software Mascot 1.9 (Matrix Science, Boston, MA) with confirmatory or complementary analyses with TurboSequest of the Bioworks Browser 3.2, build 41 (ThermoFinnigan, Madison, CT). Tyrosine (+ 45 Da) and methionine (+16 Da) of each MS/MS spectrum was analysed as specific nitration and oxidation, respectively. F_1-ATPase amino acid numbering is based on NCBI sequence NP_599191 and the structure shown in Figure 3 was generated with the WebLab Viewer Pro 3.7 (Molecular Simulations, Inc., San Diego, CA) from the Protein Data Bank (Structure explorer, 1BMF) based on the F_1-ATPase crystal structure [25].

Measurement of enzyme activities

Succinyl-CoA-transferase (SCOT) activity was measured as described [26]: mitochondria were disrupted by sonication and then centrifuged at 10 000 *g* for 20 min. The supernatant was incubated in a 50 mM Tris-HCl buffer, pH 8.0, containing 5 mM $MgCl_2$, 4 mM iodoacetamide, 0.2 mM acetoacetate and 0.1 mM succinyl-CoA. Activity was measured spectrophotometrically at 313 nm. Complex IV (cytochrome oxidase) activity was measured using a MitoProfile Assay Kit (Mitosciences, Eugene, OR) according to manufacturer's instructions. Complex IV was immunocaptured with cytochrome oxidase antibody and the activity was measured by the oxidation of reduced cytochome *c* at 550 nm ($\varepsilon = 21$ mM^{-1} cm^{-1}). ATPase (complex V) activity was measured in purified mitochondria from rat brain: 50 μg of broken mitochondria were added to 1 ml reaction buffer containing 250 mM sucrose, 50 mM HEPES, pH 8.0, 5 mM $MgSO_4$, 2.5 mM sodium phosphoenolpyruvate, 2 μg antimycin, 5 ml of PK/LDH mixture and 2.5 mM ATP. Reaction was initiated by addition of 0.35 mM NADH and initial rates were measured at 340 nm at 25°C ($\varepsilon_{340} = 6.22$ mM^{-1} cm^{-1}). Protein levels of SCOT and F_1-ATPase were assessed by immunoblotting using specific antibodies against SCOT (Novus, Littleton, CO) and F_1-ATPase (Santa Cruz Biotech, Santa Cruz, CA).

Polarographic assays

Oxygen consumption was measured with a Clark-type electrode (Hansatech, UK) assembled to a thermostatic water jacket. The assay buffer consisted of 100 mM KCl, 75 mM mannitol, 25 mM sucrose, 5 mM KH_2PO_4, 5 mM $MgCl_2$, 0.05 mM EDTA, 20 mM HEPES, pH 7.4. The mitochondrial suspension was maintained under continuous stirring with a magnetic agitator in the electrode chamber. State 4 respiration was measured with complex I substrates (2.5 mM pyruvate + 2.5 mM malate) and state 3 respiration in the presence of 350 μM ADP.

Statistical analysis

Data are reported as means ± SD of at least six independent experiments. Significant differences between mean values were determined by Student *t*-test. Means were considered to be statistically significant if $p < 0.05$.

Results

Rat brain nNOS protein level is elevated during ageing

The total nNOS content in rat brain homogenate increased during ageing, as detected by Western blot using an antibody targeting the C-terminal of nNOS (BD Biosciences, Cat # 610308). A specific nNOS band with a molecular weight ~155 KDa, which corresponds to the cytosolic form of nNOS [12], was observed. After normalizing with β-actin, the level of nNOS was found to be elevated ~2-fold in 26 month-old rats as compared to 6 month-old rats (Figure 1). Furthermore, regardless of whether antibody targeting either N- or C-terminal of brain NOS was used, mitochondrial NOS (mtNOS, 144 kDa) was not detected in isolated mitochondria from Fisher rat brains (data not shown). The existence of mtNOS has been reported in experiments using Wistar rats [12], thus suggesting that the expression of mtNOS is strain-specific.

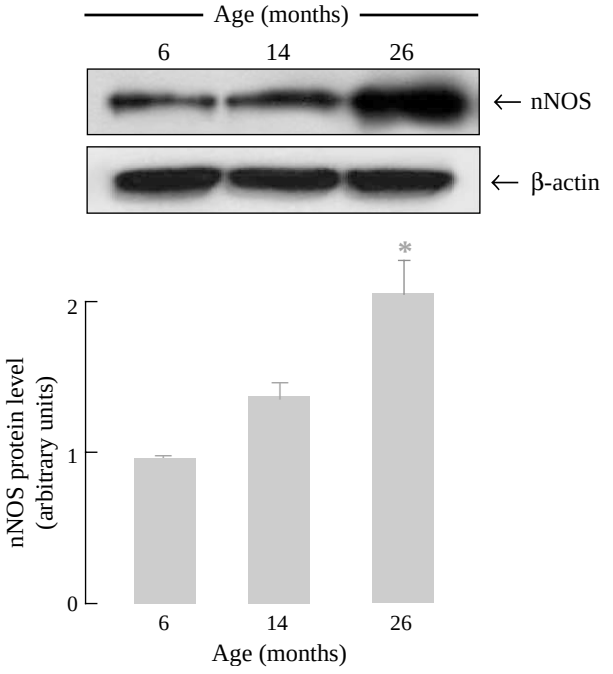

Figure 1. Increase of nNOS protein content in rat brain during ageing. Representative western blots of total brain homogenate obtained from Fisher 344 rats at 6, 14 and 26 months of age. The nNOS protein in the cell homogenate was detected by using the α-nNOS antibody. The intensity of nNOS bands were quantified and calculated against β-actin levels using a Versa Doc imaging system (Bio-Rad). $n=9$, $^{\star}p<0.05$.

Increased mitochondrial protein nitration level during ageing

The elevated nNOS levels as a function of age were accompanied by increased level of protein nitration in mitochondria, assessed by immunoblotting. Nitration was detected in the mitochondrial fraction (Figure 2) but not in the cytosolic fraction, thus supporting the notion that mitochondria are major cellular sources of $O_2^{\bullet}$ and, hence, they set a favourable environment for $ONOO^-$ formation. No band was detected after incubating the same membrane with 1 mM dithionite, indicating the specificity of the anti-nitrotyrosine antibody (data not shown). Nitration of mitochondrial proteins increased during ageing. Only a few mitochondrial proteins containing nitrotyrosine were detected (Figure 2). This suggests that nitration is limited to a number of mitochondrial proteins, thus implying a specific age-dependent functional impairment of these proteins.

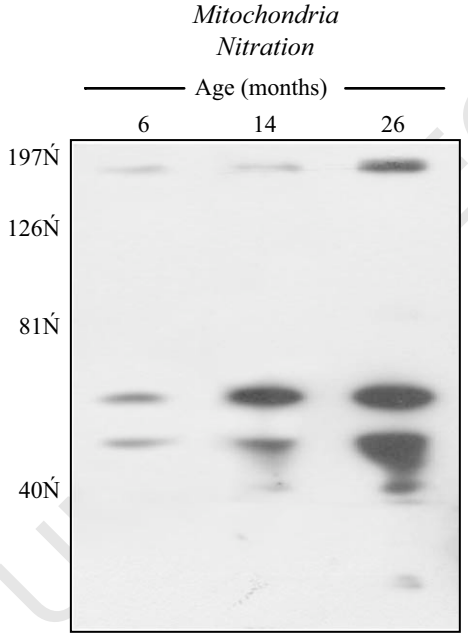

Figure 2. Increase of nitrosylation and nitration of rat brain cytosolic and mitochondrial proteins during ageing. Rat brains at 6, 14 and 26 months of age were immunoblotted for the assay of protein nitration. Nitrotyrosine in the mitochondrial fraction was detected by the α-nitrotyrosine antibody.

Succinyl-CoA-transferase and F_1-ATPase are nitrated during ageing

The nitrotyrosine immunoreactive 58 kDa proteins that were isolated from rat brain mitochondria were immuno-precipitated by anti-nitrotyrosine antibody and subjected to LC/MS/MS analyses. The mitochondrial enzymes succinyl-CoA-transferase (SCOT) and F_1-ATPase (Complex V) were identified as these nitrated proteins (Figure 3 and Tables I and II). The sequence coverage for SCOT and F_1-ATPase are 24% and 26%, respectively. The site of nitration of F_1-ATPase was identified as Tyr^{269} of the β sub-unit (Figure 3 and Tables I and II). 3D mapping of Tyr^{269} was based on the crystal structure of bovine ATPase, which shared high sequence similarity for comparison purposes (Figure 3). The nitrated tyrosine appears to be at the periphery of the active site and carbon three (position of nitration) is relatively close ($\sim$10 Å) to the Mg^{2+} ion associated with the catalytic core (Figure 3B and C). It is surmised that the increased production of $^{\bullet}NO$ by cytosolic nNOS and diffusion into the mitochondria, a compartment with higher $O_2^{\bullet -}$ concentration and a more favourable site for $ONOO^-$ formation, results in the specific nitration of both SCOT and F_1-ATPase.

Upon analysis of the observed peptides in F_1-ATPase, the nitrated VALVYGQMNEPPGAR peptide was found. Tyrosine residue of this particular peptide is located in the catalytic pocket. Total mass of the peptide (mass $+16$ and $+45$ Da for methionine oxidation and tyrosine nitration) corresponded with the sequence and multiple MS2 spectra for different y- and b-ion masses (Figure 3A). Peptide ions Y_5 and B_{10} (Figure 3A and Table II) ionized well for the peptide. Other spectra also showed significant intensity of tyrosine nitration (Figure 3A and Table II) and it is noted that Y_{11}, Y_{13}^{++}, B_8, B_9, B_{13}, and B_{14} all demonstrate the presence of nitrotyrosine ($+45$ Da). These findings support the occurrence of tyrosine nitration on the

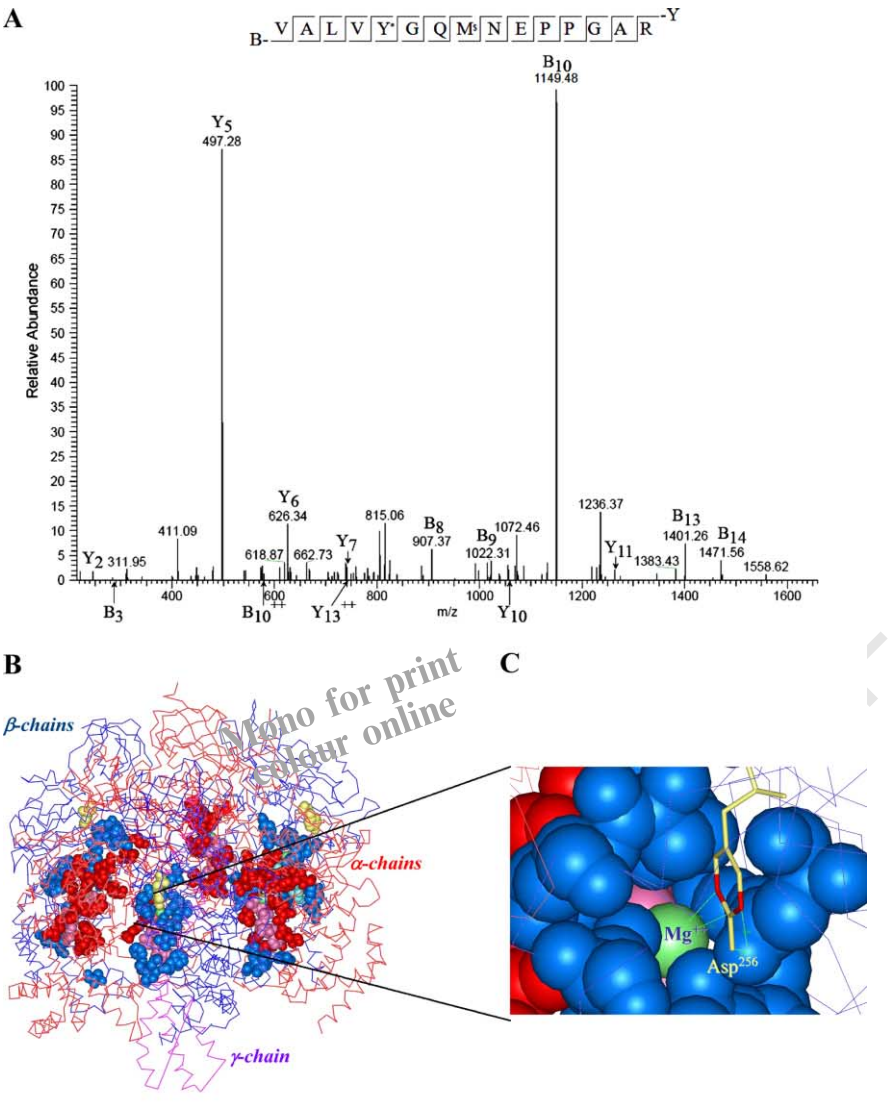

D

Nitration of Tyr^{269} of ATPase β-subunit

Tryptic peptide	residue	Xc	Δcn
VALV**Y**GQMNEPPGAR Nitro(Y)	Tyr^{269}	2.509	0.188
VALV**Y**GQMNEPPGAR Nitro(Y)	Tyr^{269}	2.876	0.293
VALV**Y**GQMNEPPGAR Nitro(Y)	Tyr^{269}	2.269	0.349

Figure 3. Succinyl-CoA-transferase and F_1-ATPase β sub-unit identified as nitration targets by LC/MS/MS during ageing. The ATP synthase β-sub-unit was identified by LC/MS/MS and was found to be nitrated on Tyr^{269}, as mentioned in the Materials and methods and Result sections. (A) MS spectrum of nitrated peptide from ATP synthase (*, +45 Da, $, +16 Da for Y and M, respectively; see Table II). (B) 3D mapping of Tyr^{269} in the protein and (C) magnification of the active site from the crystal structure of bovine F_1-ATPase. Components and their corresponding colours: α-chains (red); β-chains (blue); γ-chain (purple); F_1-α active site residues (red); F_1-β active site residues (blue); Mg^{2+} (green); ANP (violet); ADP (turquoise) and nitrotyrosine 269 (yellow, 219 in crystal structure). (D) Sequest scores of nitrated peptide of F_1-ATP synthase β sub-unit.

peptide, further confirmed by Sequest scores (Xc and $\triangle$cn) (Figure 3D).

It is worth noting that the mitochondrial protein nitration pattern in *in vitro* and *in vivo* models differ substantially: on the one hand, when isolated mitochondria are treated with $ONOO^-$, a multitude of 3-nitrotyrosine positive bands are observed [27]. On the other hand, in normal ageing, as the experimental model used in this study, the increases in cytosolic nNOS activity leads to a discreet and specific mitochondrial nitration pattern, as shown in Figure 2.

Table I. LC/MS/MS analyses of Succinyl-CoA-transferase and F_1-ATPase.

Tryptic peptide	Xc	Δcn
Succinyl-CoA-transferase[a]		
DGSVAIASKPR	2.424	0.365
FYTDPVEAVK	2.328	0.315
GMGGAMDLVSSSK	4.224	0.514
YGDLANWMIPGK	4.952	0.639
GGHVNLTMLGAMQVSK	3.444	0.108
AGGAGVPAFYTSTGYGTLVQEGGSPIK	4.926	0.540
F_1-ATPase[b]		
TIAMDGTEGLVR	3.555	0.462
VLDSGAPIK	3.018	0.269
VLDSGAPIKIPVGPETLGR	4.068	0.447
IPVGPETLGR	3.283	0.541
IMNVIGEPIDER	3.993	0.785
VVDLLAPYK	3.708	0.426
IGLFGGAGVGK	2.949	0.361
TVLIMELINNVAK	4.547	0.406
VALVYGQMNEPPGAR	4.222	0.465
FTQAGSEVSALLGR	5.146	0.550
IPSAVGYQPTLATDMGTMQER	5.179	0.297

[a]50 total SCOT high quality peptides (six unique) were identified by LC/MS/MS (Mascot scores ranged from 37–73).
[b]80 total F_1-ATPase β-chain high quality peptides (11 unique) were identified by LC/MS/MS (Mascot scores ranged from 30–94).

Nitration compromises succinyl-CoA-transferase and F_1-ATPase activities

Although the protein levels of both SCOT and F_1-ATPase remained unchanged with age, their activities following nitration were significantly decreased (Figure 4A and B). It is well documented that cytochrome oxidase (complex IV) activity, the terminal electron acceptor of the mitochondrial electron-transfer chain, decreases with ageing [26], a fact that is illustrated by Figure 4C and D. The decline in cytochrome oxidase activity was less pronounced than that of SCOT and F_1-ATPase (Figure 4D). The age-dependent decline in SCOT and F_1-ATPase activities suggests that these enzymes may become rate limiting, thereby affecting energy metabolism. Moreover, the age-dependent decline in SCOT activity implies a less efficient ketone body metabolism as an energy source in the brain. Thus, the age-dependent decline in SCOT activity may become more detrimental if simultaneously coupled to an impaired glucose metabolism.

Overall mitochondrial function and ageing

The respiratory control ratios (RCR) of brain mitochondria respiring on complex I substrates (malate/glutamate) were decreased as a function of age (Table III): a 25% decrease in oxidative phosphorylation efficiency was observed in 26-month old animals as compared with 6-month old rats. The lower RCR values were accounted for largely by an increase in state 4 respiration, with state 3 respiration remaining somehow constant with age (Table III). The P:O ratio was $\sim$20% lower in 26-month old animals as compared with the young animals (6-month old).

Compromised energy production enhanced cytochrome c release

The compromised energy metabolism as a function of age referred to above was associated with a decrease in mitochondrial cytochrome *c* and corresponding increases in the cytosolic levels of the same hemoprotein (Figure 5). This establishes a link between impaired energy metabolism and mitochondrion-driven apoptosis.

Table II. Theoretical masses of nitrated ATPase peptides from MS2 spectrum.

		Modifications M+16 Da and Y +45 Da					
	N°	b mass	b^{++} mass	y mass	y^{++} mass	N°	
V	1	100.0763	50.038 14	1662.811	831.405 5	15	V
A	2	171.1134	85.556 7	1563.743	781.871 3	14	A
L	3	284.1975	142.098 7	1492.706	746.352 8	13	L
V	4	383.2659	191.632 9	1379.621	689.810 7	12	V
Y	5	591.3292	295.664 6	1280.553	640.276 5	11	Y
G	6	648.3507	324.175 3	1072.49	536.244 9	10	G
Q	7	776.4092	388.204 6	1015.468	507.734 1	9	Q
M	8	923.4497	461.724 9	887.4097	443.704 8	8	M
N	9	1037.493	518.746 3	740.3692	370.184 6	7	N
E	10	1166.535	583.267 6	626.3262	313.163 1	6	E
P	11	1263.588	631.794	497.2837	248.641 8	5	P
P	12	1360.641	680.320 4	400.2309	200.115 4	4	P
G	13	1417.662	708.831 1	303.1781	151.589 1	3	G
A	14	1488.699	744.349 7	246.1567	123.078 3	2	A
R	15	1644.8	822.400 2	175.1196	87.559 78	1	R

Y⋆ (tyrosine) +45 and $M^{\$}$ (methionine) +16 Da for nitrated VALVY⋆GQ$M^{\$}$N EPPGAR are shown and observed peptides are shown in italic that are within 0.8 Da of the theoretical mass. Observed masses for the nitrated peptide are annotated in Figure 3A.

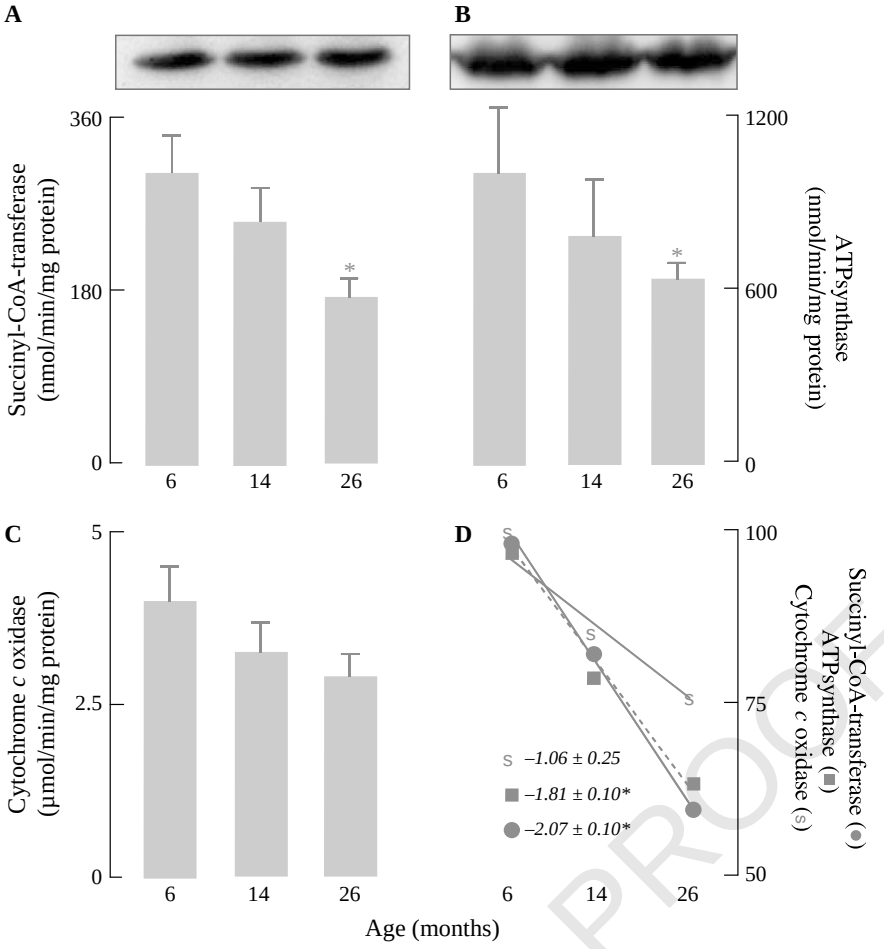

Figure 4. Succinyl-CoA-transferase and ATPase activities during ageing. The enzymatic activities of (A) SCOT and (B) F_1-ATPase were significantly decreased during ageing. Top panels indicate that protein levels were unchanged. (C) A moderate decline of cytochrome oxidase activity was observed during ageing. (D) Comparison of the effect of ageing on the declines of enzymatic activities: SCOT (●, solid line; slope −2.07); ATP synthase (■, broken line; slope −1.81) and cytochrome oxidase (▲, solid line; slope −1.06). The slopes in D indicate that the reduction of SCOT and ATP synthase activities were more pronounced than that of cytochrome oxidase. $n=9$, $\star$ $p<0.05$.

Discussion

•NO produced in the central nervous system can be neuroprotective or neurotoxic [2,28]. Neuronal nitric oxide synthase (nNOS) is the Ca^{2+}-calmodulin-dependent NOS isoform that is constitutively expressed in all brain cell types including neurons, astrocytes and glial cells. Excessive formation of •NO as either in excitotoxicity (excessive activation of NMDA receptor with concomitant glutamate release) or induction of nitric oxide synthase in astrocytes and microglial cells (as a response to pro-inflammatory stimuli) is likely involved in the pathophysiology of age-related neurodegenerative disorders, such as Alzheimer's and Parkinson's diseases [29].

Table III. Respiratory function of rat whole brain mitochondria in ageing.

	State 3	State 4		
Age (months)	ng at O/min/mg protein		RCR	P:O
6	35.6±1.6	5.2±0.3	6.8±0.3	2.92±0.60
14	32.8±1.6$\star$	5.5±0.3	5.9±1.5	2.61±0.62
26	35.5±2.1	6.9±0.1$\star$	5.1±0.3$\star$	2.40±0.56

$\star p<0.05$, $n=9$.

This study recognized that the expression of cytosolic nNOS increases with age and this is associated with increased and specific patterns of nitration of mitochondrial proteins. This modification is expected, because mitochondria are major cellular sources of $O_2^{\bullet -}$, thus providing an adequate setting for $ONOO^-$ formation. Due to its short half-life, its high chemical reactivity and its electrical charge, it is unlikely that mitochondrial $ONOO^-$ would be able to diffuse to the cytosol and be involved in the nitration of cytosolic proteins. Under conditions of enhanced •NO and $O_2^{\bullet -}$ production in the mitochondrial compartment, •NO can outcompete Mn-superoxide dismutase for $O_2^{\bullet -}$ [30], thus resulting in $ONOO^-$ formation and mitochondrial protein nitration.

The catalytic activities of brain SCOT and F_1-ATPase are compromised by nitration during ageing. SCOT mediates the rate-determining step of ketolysis

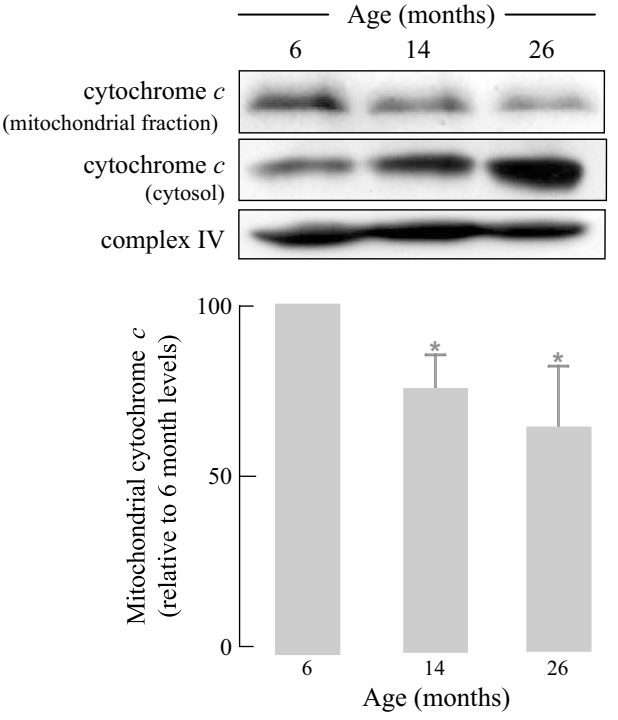

Figure 5. Increased mitochondrial cytochrome *c* release during ageing. Mitochondrial and cytosolic fractions of rat brain from different rat ages were collected and subjected to immunoblotting using the anti-cytochrome *c* antibody. Mitochondrial cytochrome *c* decreased with age with a corresponding increase in cytosolic cytochrome *c*. Cytochrome oxidase staining was included as a loading control. $n=9$, $^{\star}p<0.05$.

in extrahepatic tissues by conversing ketone bodies into acetoacetyl-CoA, which subsequently enters the citric acid cycle for energy production. In the brain, ketone bodies are the only alternative—but importantly—energy source during periods of glucose deficiency. Ketone bodies have been suggested to help rescue mitochondrial respiration in Parkinson's disease models by increasing succinate generation, which involves SCOT-mediated catalysis and bypasses the presumed complex I deficiency by boosting mitochondrial function and ATP production [31,32]. Thus, nitration of SCOT as a function of age renders the brain more susceptible to an energy crisis, especially in the case of age-associated type II diabetes due to the compounding effect of impaired glucose and ketone body utilization. The SCOT activity in the heart has been reported to increase during ageing due to nitration of a tryptophan residue [33]. The reason for this discrepancy can be partly explained by the facts that (i) nitration occurred on different residue: tryptophan residues in heart but tyrosine in brain; and (ii) the heart is the main ketone body-utilizing organ, whereas the brain only utilizes ketone bodies as an alternative backup energy source.

This is the first study showing the F_1-ATPase is being nitrated at Tyr^{269} during ageing with a compromised catalytic activity. 3D mapping of Tyr^{269} in F_1-ATPase (Figure 3) suggests deficient ADP binding to the active site, thus lowering the ATP production rate. However, the sequence coverage of F_1-ATPase is only 26%, thus suggesting that there may be other potential nitration sites yet to be determined.

Of note, the declines in the activities of SCOT and F_1-ATPase with age were due to $^{\bullet}NO$-mediated protein post-translational modifications (nitration), whereas the lower decline in cytochrome oxidase (complex IV) activity may be ascribed to a decreased expression (and possibly assembly) of the enzyme. In addition, it is interesting to note that $^{\bullet}NO$ binds to the enzyme complex IV and inhibits rapidly (seconds or faster) its activity at ratios of O_2 to $^{\bullet}NO$ in the 40–500 range. However, the increased cytosolic nNOS activity reported here would be able to elicit a physiological cytochrome oxidase inhibition. The levels of cytochrome oxidase found in cells seem to be optimized to allow a moderate but not excessive overlap between the signalling roles of $^{\bullet}NO$ and the inhibition of state 3 mitochondrial respiration by $^{\bullet}NO$ [34], but the increase of nNOS with ageing seems to augment the magnitude of this overlap. The inhibition of cytochrome oxidase by $^{\bullet}NO$ is also associated with an increase in $O_2^{\bullet -}$ generation at complex III sites and optimizes the setting for $ONOO^-$-dependent protein nitration [3].

The cytochrome *c* release observed as a function of age correlated with the increase in cytosolic nNOS activity and may be ascribed to excessive formation of $ONOO^-$ in mitochondria. It is well documented that $ONOO^-$ can induce both necrotic and apoptotic cell death which eventually leads to neurodegeneration [35].

Acknowledgements

Supported by NIH grant RO1 AG016718.

Declaration of interest: The authors report no conflicts of interest. The authors alone are responsible for the content and writing of the paper.

References

[1] Beckman JS. The physiological and pathological chemistry of nitric oxide. In: Lancaster J, editor. Nitric oxide: Principles and actions. San Diego: Academic Press; 1996. p 1–82.

[2] Calabrese V, Mancuso C, Calvani M, Frizzarelli E, Butterfield DA, Stella AM. Nitric oxide in the central nervous system: neuroprotection versus neurotoxicity. Nature Rev Neurosci 2007;8:766–775.

[3] Moncada S, Bolaños JP. Nitric oxide, cell bioenergetics and neurodegeneration. J Neurochem 2006;97:1676–1689.

[4] McCann SM. The nitric oxide hypothesis of brain aging. Exp Gerontol 1997;32:431–440.

[5] Vernet D, Bonavera JJ, Swerdloff RS, Gonzalez-Cadavid NF, Wang C. Spontaneous expression of inducible nitric oxide synthase in the hypothalamus and other brain regions of aging rats. Endocrinology 1998;139:3254–3261.

[6] Jurado S, Sanchez-Prieto J, Torres M. Expression of cGMP-dependent protein kinases (I and II) and neuronal nitric oxide synthase in the developing rat cerebellum. Brain Res Bull 2005;65:111–115.

[7] Brown GC, Cooper CE. Nanomolar concentrations of nitric oxide reversibly inhibit synaptosomal respiration by competing with oxygen at cytochrome oxidase. FEBS Lett 1994;356: 295–298.

[8] Derakhshan B, Hao G, Gross SS. Balancing reactivity against selectivity: the evolution of protein S-nitrosylation as an effector of cell signaling by nitric oxide. Cardiovasc Res 2007; 75:210–219.

[9] Davis KL, Martin E, Turko IV, Murad F. Novel effects of nitric oxide. Annu Rev Pharmacol Toxicol 2001;41:203–236.

[10] Boveris A, Costa LE, Poderoso JJ, Carreras MC, Cadenas E. Regulation of mitochondrial respiration by oxygen and nitric oxide. Ann NY Acad Sci 2000;899:121–135.

[11] Valdéz LB, Zaobornyj T, Boveris A. Mitochondrial metabolic states and membrane potential modulate mtNOS activity. Biochim Biophys Acta 2006;1757:166–172.

[12] Riobó N, Melani M, Sanjuan N, Fiszman ML, Gravielle MC, Carreras MC, Cadenas E, Poderoso JJ. The modulation of mitochondrial nitric oxide synthase activity in rat brain development. J Biol Chem 2002;277:42447–42455.

[13] Beckman JS, Beckman TW, Chen J, Marshall PA, Freeman BA. Apparent hydroxyl radical production by peroxynitrite: implications for endothelial injury from nitric oxide and superoxide. Proc Natl Acad Sci USA 1990;87:1620–1624.

[14] Boveris A, Cadenas E Cellular sources and steady-state levels of reactive oxygen species. In: Clerch LB, Massaro DJ, editors. Oxygen, gene expression, and cellular function. New York: Marcel Dekker; 1997. p 1–25.

[15] Valdéz L, Alvarez S, Lores Arnáiz S, Schöpfer F, Boveris A. Reactions of peroxynitrite in the mitochondrial matrix. Free Radic Biol Med 2000;29:349–356.

[16] Schopfer F, Riobo NA, Carreras MC, Alvarez B, Radi R, Boveris A, Cadenas E, Poderoso JJ. Oxidation of ubiquinol by peroxynitrite: implications for protection of mitochondria against nitrosative damage. Biochem J 2000;349:35–42.

[17] Bharath S, Andersen JK. Glutathione depletion in a midbrain-derived immortalized dopaminergic cell line results in limited tyrosine nitration of mitochondrial complex I subunits: implications for Parkinson's disease. Antioxid Redox Signal 2005;7:900–910.

[18] Konorev EA, Hogg N, Kalyanaraman B. Rapid and irreversible inhibition of creatine kinase by peroxynitrite. FEBS Lett 1998;427:171–174.

[19] Han D, Canali R, Garcia J, Aguilera R, Gallaher TK, Cadenas E. Sites and mechanisms of aconitase inactivation by peroxynitrite: modulation by citrate and glutathione. Biochemistry 2005;44:11986–11996.

[20] Murray J, Taylor SW, Zhang B, Ghosh SS, Capaldi RA. Oxidative damage to mitochondrial complex I due to peroxynitrite: identification of reactive tyrosines by mass spectrometry. J Biol Chem 2003;278:37223–37230.

[21] Mannick JB. Regulation of apoptosis by protein S-nitrosylation. Amino Acids 2007;32:523–526.

[22] Stewart VC, Sharpe MA, Clark JB, Heales SJ. Astrocyte-derived nitric oxide causes both reversible and irreversible damage to the neuronal mitochondrial respiratory chain. J Neurochem 2000;75:694–700.

[23] Cooper CE, Davies NA, Psychoulis M, Canevari L, Bates TE, Dobbie MS, Casley CS, Sharpe MA. Nitric oxide and peroxynitrite cause irreversible increases in the K(m) for oxygen of mitochondrial cytochrome oxidase: in vitro and in vivo studies. Biochim Biophys Acta 2003;1607:27–34.

[24] Han D, Williams E, Cadenas E. Mitochondrial respiratory chain-dependent generation of superoxide anion and its release into the intermembrane space. Biochem J 2001;353: 411–416.

[25] Abrahams JP, Leslie AG, Lutter R, Walker JE. Structure at 2.8 Å resolution of F1-ATPase from bovine heart mitochondria. Nature 1994;370:621–628.

[26] Williamson DH, Bates MW, Page MA, Krebs HA. Activities of enzymes involved in acetoacetate utilization in adult mammalian tissues. Biochem J 1971;121:41–47.

[27] Riobó NA, Clementi E, Melani M, Boveris A, Cadenas E, Moncada S, Poderoso JJ. Nitric oxide inhibits mitochondrial NADH-ubiquinone reductase activity through the formation of peroxynitrite. Biochem J 2001;359:139–145.

[28] Estevez AG, Kamaid A, Thompson JA, Cornwell TL, Radi R, Barbeito L, Beckman JS. Cyclic guanosine 5' monophosphate (GMP) prevents expression of neuronal nitric oxide synthase and apoptosis in motor neurons deprived of trophic factors in rats. Neurosci Lett 2002;326:201–205.

[29] Dawson VL, Dawson TM. Nitric oxide in neurodegeneration. Prog Brain Res 1998;118:215–229.

[30] Beckman J, Koppenol WH. Nitric oxide, superoxide, and peroxynitrite: the good, the bad, and the ugly. Am J Physiol 1996;261:H590–H597.

[31] Kashiwaya Y, Takeshima T, Mori N, Nakashima K, Clarke K, Veech RL. D-beta-hydroxybutyrate protects neurons in models of Alzheimer's and Parkinson's disease. Proc Natl Acad Sci USA 2000;97:5440–5444.

[32] Tieu K, Perier C, Caspersen C, Teismann P, Wu DC, Yan SD, Naini A, Vila M, Jackson-Lewis V, Ramasamy R, Przedborski S. D-beta-hydroxybutyrate rescues mitochondrial respiration and mitigates features of Parkinson disease. J Clin Invest 2003;112:892–901.

[33] Rebrin I, Brégère C, Kamzalov S, Gallaher TK, Sohal RS. Nitration of tryptophan 372 in succinyl-CoA:3-ketoacid CoA transferase during aging in rat heart mitochondria. Biochemistry 2007;46:10130–10144.

[34] Antunes F, Boveris A, Cadenas E. On the mechanism and biology of cytochrome oxidase inhibition by nitric oxide. Proc Natl Acad Sci USA 2004;101:16774–16779.

[35] Heales SJ, Bolanos JP, Stewart VC, Brookes PS, Land JM, Clark JB. Nitric oxide, mitochondria and neurological disease. Biochim Biophys Acta 1999;1410:215–228.